Proc. Instn Civ. Engrs, Part 2, 1975, **59**, Dec., 645–658

7806 An analysis of the failure mechanism of an axially loaded simply supported steel plate

P. DAVIES, BSc(Eng)*
K. O. KEMP, BSc(Eng), PhD, MICE, MIStructEng*
A. C. WALKER, MSc, PhD, MIMechE*

Tests on unstiffened and stiffened steel plates under uniaxial compression have shown that the attainment of ultimate load is closely followed by yielding of a localized portion of the plate. The yield lines form in a consistent pattern and post-failure deflexions are governed by the behaviour of this plastic mechanism. A rigid–plastic analysis of an idealized form of this mechanism is presented which employs a Tresca yield criterion for evaluation of stresses in the plastic zone; an approximation of this criterion is used to obtain a simple load–deflexion equation for low and medium b/t ratios. The importance of shearing forces in determining the shape and load–deflexion behaviour of the mechanism is demonstrated and the consequent necessity for inclusion in the yield criterion is shown. The theoretical unloading curve is in good agreement with experimental results and gives a close approximation to the failure load by intersection with an elastic loading curve. The results indicate that development of this form of analysis may lead not only to a good estimation of the behaviour of plate at failure, but also to the load-shedding characteristics of interrelated elements in a structure.

Introduction

A principal objective of the analysis of a structure is to determine its ultimate carrying capacity. Generally the engineering approach subdivides the structure into its constituent parts and analyses each element in an attempt to find the individual ultimate load capacities. Consequently, much research has centred on the behaviour of simply supported unstiffened steel plates as these form a large part of many steel structures. In particular, the behaviour of rectangular plates subjected to uniaxial compression has received a great deal of attention, partly because of the fundamental nature of the loading but more because the flanges of beams and girders are predominantly subjected to it.

2. The behaviour of a steel plate at failure presents a formidable analytical problem because of the complex elasto-plastic behaviour of the material with its ensuing rapidly changing deflexion characteristics. Traditionally, estimations of ultimate load-carrying capacity have been largely empirical with more recent emphasis on semi-empirical formulations based on the elastic critical

Written discussion closes 16 February, 1976, for publication in *Proceedings*, Part 2.
* Department of Civil and Municipal Engineering, University College London.

Notation

b	breadth of plate
d	depth of neutral axis below mid-plane
l	length of mechanism
M	yield bending moment per unit length of yield line
M_0	M with zero axial and shearing forces
N	yield axial force at mid-depth per unit length of yield line
N_0	N with zero bending and shearing forces
P	total axial load on plate
S	yield shearing force per unit length of yield line
S_0	S with zero bending and axial forces
t	thickness of plate
w	out of plane deflexion of central yield line
w_0	pre-failure value of w
w'	post-failure value of w
β	shape angle of mechanism
σ	normal stress on yield line
σ^*	average stress across width of plate normalized with respect to yield stress
σ_y	yield stress
τ	shear stress on yield line

load of the plate. Attempts have been made to study the elasto-plastic behaviour, particularly by Graves-Smith,[1] Moxham[2] and Crisfield.[3] These approaches are of a numerical nature involving large computer programs for the solution of finite element or finite difference equations.

3. Elements of a structure under different loading and edge conditions may fail with the formation of various yield shapes or mechanisms, and plastic analyses have been used to investigate their behaviour.

4. Dean[4] studied the failure of a stiffened box girder diaphragm using a mechanism approach; Rockey and Skaloud[5] and Calladine[6] have used rigid plastic analyses for calculating the collapse loads of plate girder webs under high shearing forces.

5. Examination of a large number of experimentally tested unstiffened and stiffened plates under uniaxial compression (Figs 1 and 2) indicates that failure occurs with yielding of a localized portion of the plate, the form of which appears surprisingly well defined and consistent. The possibility of analysis of this plastic mechanism has been recognized by Sherbourne and Korol,[7] Walker and Murray[8] and Murray.[9,10] This rigid perfectly plastic analysis results in the prediction of an unloading line on the load–deflexion plot, which gives not only an estimate of the failure load (by intersection with an elastic loading line) but also an indication of the degree of violence or instability associated with the load-shedding at failure.

6. These analyses of this plate mechanism are based on an equilibrium approach in which it is assumed that longitudinal elemental strips of the plastic mechanism could act independently of the other portions of the plate. Only direct and bending stress actions were included in the analysis of the strip, although Murray[10] in the determination of the large deflexion behaviour drew attention to the presence of large shear stresses in the mechanism. The principal advantage of this type of analysis is that it results in simple, easily

applied formulations. Although the results of these analyses show inconsistencies when compared with published test data, it is probable that this is because of the simplifying assumptions in the analyses rather than any basic inability of the plastic mechanism approach to model adequately the real behaviour of a plate after failure.

7. The Paper contributes to the development of the yield line approach by presenting an analysis in which shear is included in the stress system at the plastic zone.

Fig. 1

Fig. 2

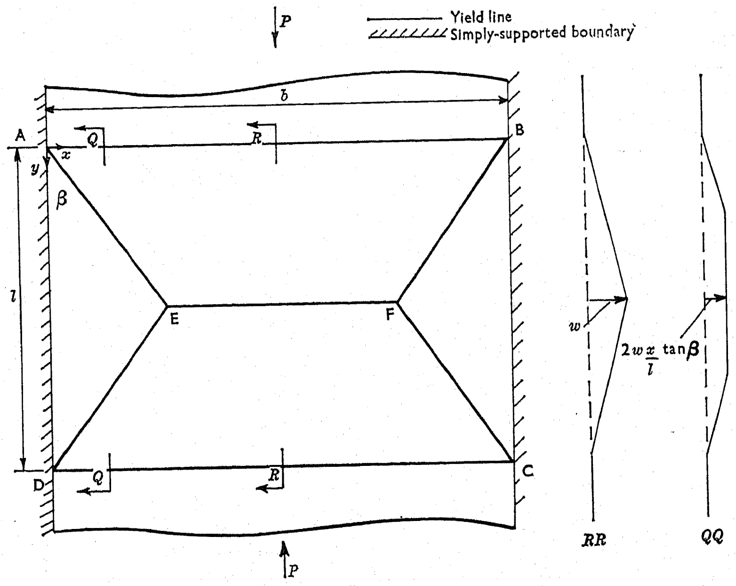

Fig. 3. Plastic mechanism

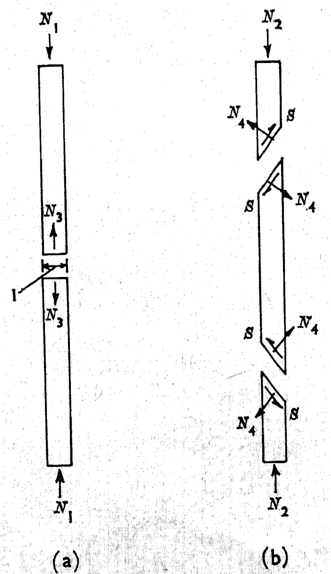

Fig. 4. Characteristic strips with forces acting; (a) mid-zone unit strip, (b) edge zone unit strip

Mechanism

8. The failure mechanism of a rectangular steel plate under axial compression may be approximated for analysis to a pitched roof mechanism of the form shown in Fig. 3, with all zones of yielding represented by straight yield lines. The mechanism is assumed to form in the length of a long, simply supported plate, the length and shape of the mechanism being described by the two parameters l and β respectively. The plastic hinges or yield lines are assumed to form under the influence of a bending moment M, a compressive axial (membrane) force N acting at the mid-plane of the plate and a shearing force S acting uniformly over the thickness of plate t.

9. The behaviour of this mechanism as the central deflexion w grows may be analysed by considering the plate to be made up of a number of strips which are free to slide in relation to each other, all work being done at the yield lines. The mechanism of Fig. 3 has two characteristic unit strips: one at the central region and one at the outer region of the plate. These characteristic strips are shown in Fig. 4 with the forces acting on them.

Yield criterion

10. On a yield line the bending, normal and shearing forces are related by a yield criterion. At any point in the depth of the plate the relationship between the normal and shearing stresses is assumed to be given by the Tresca yield criterion

$$\sigma^2+4\tau^2 = \sigma_y^2 \quad . \quad . \quad . \quad . \quad . \quad . \quad . \quad (1)$$

With reference to Fig. 5, the membrane force N per unit length of yield line is

$$N = \sigma\left(\frac{t}{2}+d\right) - \sigma\left(\frac{t}{2}-d\right) = 2d\sigma \quad . \quad . \quad . \quad . \quad (2)$$

and the moment per unit length of yield line is

$$M = \frac{\sigma}{2}\left(\frac{t}{2}+d\right)\left(\frac{t}{2}-d\right) + \frac{\sigma}{2}\left(\frac{t}{2}-d\right)\left(\frac{t}{2}+d\right) = \frac{\sigma}{4}t^2\left\{1-\left(\frac{2d}{t}\right)^2\right\} \quad . \quad (3)$$

Elimination of σ and d in equations (1)–(3) gives the yield criterion in terms of the moment and forces on the section

$$\frac{M}{M_0}\left\{1-\left(\frac{S}{S_0}\right)^2\right\}^{\frac{1}{2}} + \left(\frac{N}{N_0}\right)^2 + \left(\frac{S}{S_0}\right)^2 = 1 \quad . \quad . \quad . \quad (4)$$

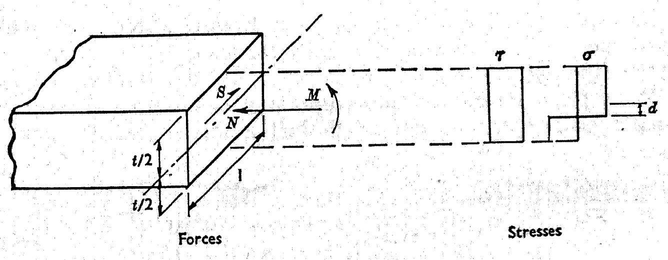

Fig. 5. Section on yield line

where $M_0 \equiv \sigma_y t^2/4$, $N_0 \equiv \sigma_y t$, $S_0 \equiv \sigma_y t/2$, $S \equiv \tau t$. It is implied that the bending and membrane forces act normally and the shearing force acts tangentially to the yield line. If the shear stress S is small relative to S_0 equation (4) may be approximated to

$$\frac{M}{M_0}+\left(\frac{N}{N_0}\right)^2+\left(\frac{S}{S_0}\right)^2 = 1 \quad . \quad . \quad . \quad . \quad . \quad (5)$$

The validity of this assumption is examined later but, because of its relative simplicity, equation (5) is now used in the analysis.

Analysis

11. The mechanism is considered at an arbitrary out of plane deflexion w of the central yield line EF. Force and moment equilibrium equations may then be written for each of the two representative strips.

12. The equations for the central strip are

$$N_1 \mathrm{d}x = N_3 \mathrm{d}x \quad . \quad . \quad . \quad . \quad . \quad . \quad . \quad . \quad (6)$$

$$N_1 \mathrm{d}x w = M_1 \mathrm{d}x + M_3 \mathrm{d}x \quad . \quad . \quad . \quad . \quad . \quad . \quad (7)$$

These equations may be combined with the approximate yield criterion equation (5) with zero shear to give the loading on the mechanism in terms of the central deflexion w, i.e.

$$\frac{N_1}{N_0} = \left[\left(\frac{w}{t}\right)^2+1\right]^{1/2} - \frac{w}{t} \quad . \quad . \quad . \quad . \quad . \quad . \quad . \quad (8)$$

This loading is constant for all central strips and hence the total load (normalized with respect to the strip squash load N_0) on the central portion of the mechanism may be written as

$$N_1{}^* = \int_0^{b-l\tan\beta} \frac{N_1}{N_0}\,\mathrm{d}x = (b-l\tan\beta)\left\{\left[\left(\frac{w}{t}\right)^2+1\right]^{1/2} - \frac{w}{t}\right\} \quad . \quad (9)$$

13. Equilibrium equations for the edge strip are written in a similar manner. Force equilibrium in the y direction is

$$N_2\,\mathrm{d}x = N_4\,\mathrm{d}l \sin\beta + S\,\mathrm{d}l\cos\beta \quad . \quad . \quad . \quad . \quad . \quad (10)$$

Force equilibrium in the x direction at the inclined yield line is

$$S\,\mathrm{d}l\sin\beta = N_4\,\mathrm{d}l\cos\beta \quad . \quad . \quad . \quad . \quad . \quad . \quad (11)$$

Moment equilibrium about the inclined yield line[9] is

$$2N_2\,\mathrm{d}xw\frac{x}{l\tan\beta} = M_2\,\mathrm{d}x + M_4\,\mathrm{d}l\,\mathrm{cosec}\,\beta \quad . \quad . \quad . \quad (12)$$

14. The edge strip is not in moment equilibrium about the y axis unless twisting moments exist along the inclined yield lines, but to retain the simplicity of the strip approach these twisting moments are assumed to be zero.

15. Writing $\mathrm{d}l = \mathrm{d}x\,\mathrm{cosec}\,\beta$ and combining equations (10)–(12) with the approximate yield criterion equation (5) the loading on the edge strip N_2 may be written as

$$\frac{N_2}{N_0} = \left(\frac{1+\mathrm{cosec}^2\beta}{2+3\cos^2\beta}\right)^{1/2}\left[1+\frac{16\cot^2\beta(w/t)^2}{(2+3\cos^2\beta)(1+\mathrm{cosec}^2\beta)}\left(\frac{x}{l}\right)^2\right]^{1/2} - \frac{4\cot\beta\,(w/t)}{2+3\cos^2\beta}\left(\frac{x}{l}\right) \quad . \quad . \quad . \quad (13)$$

This loading varies across the edge strips, but the integrated effect for both edge portions of the mechanism may be written in a normalized form as

$$N_2^* = 2\int_0^{l/2\tan\beta} \frac{N_2}{N_0}\,dx = \frac{l}{2}\tan\beta\left(\frac{1+\operatorname{cosec}^2\beta}{2+3\cos^2\beta}\right)^{1/2}$$
$$\times\left[1+\frac{4(w/t)^2}{(2+3\cos^2\beta)(1+\operatorname{cosec}^2\beta)}\right]^{1/2} - \frac{l\tan\beta}{2+3\cos^2\beta}\left(\frac{w}{t}\right)$$
$$+\frac{l\tan\beta(1+\operatorname{cosec}^2\beta)}{4(w/t)}\log\left\{\frac{2w/t}{(2+3\cos^2\beta)^{1/2}(1+\operatorname{cosec}^2\beta)^{1/2}}\right.$$
$$\left.+\left[1+\frac{4(w/t)^2}{(2+3\cos^2\beta)(1+\operatorname{cosec}^2\beta)}\right]^{1/2}\right\} \quad . \quad . \quad . \quad (14)$$

Hence the total load the mechanism can support for any given deflexion w may be expressed as

$$P = N_1^* N_0 + N_2^* N_0 \quad . \quad . \quad . \quad . \quad . \quad . \quad . \quad (15)$$

where N_1^* and N_2^* are given by equations (9) and (14) respectively. Writing this load as an average stress σ^* across the width of the plate normalized with respect to the yield stress gives

$$\sigma^* = \frac{P}{\sigma_y bt} = \frac{(N_1^* + N_2^*)}{b} \quad . \quad . \quad . \quad . \quad . \quad . \quad . \quad (16)$$

Equation (16) describes the relationship between the load and the out of plate deflexion of the mechanism with σ^* being a function of β, $1/b$ and w/t.

Load–deflexion plot

16. If the plastic mechanism is assumed to form at some value of $w = w_0$, then the equilibrium equations and the load–deflexion equation (10) can be re-written with $w = w_0 + w'$, where w' is the post-failure deflexion and w_0 may be viewed as the pre-failure deformation due to the combined effect of initial imperfections and elastic strains.

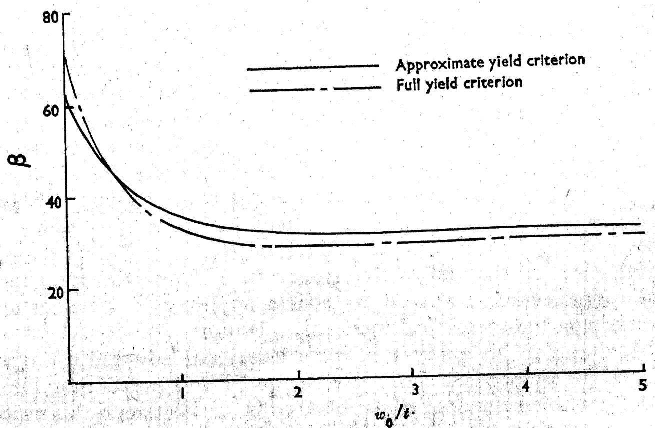

Fig. 6. Values of β for minimum σ^*

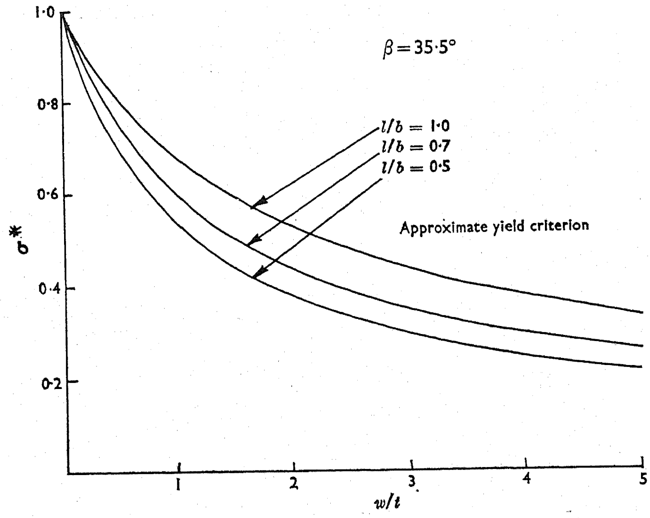

Fig. 7. Mechanism unloading lines

17. At any value of $w = w_0$, the load carried by the mechanism is minimized with respect to β to obtain the correct shape of mechanism at failure. Fig. 6 shows the values of β giving minimum values of σ^* for values of $w_0/t < 5$; these optimum values of the angle β rapidly fall to about 32° and are reasonably insensitive to variation of the length to breadth ratio of the mechanism, in the range $0{\cdot}5 < l/b < 1{\cdot}0$. However, summation of the stresses along the yield lines shows that the minimum value of β for which the inequalities implicit in the yield criteria ($M/M_0 \leqslant 1$, $N/N_0 \leqslant 1$, $S/S_0 \leqslant 1$) hold true is an angle of 35·5°. This value is therefore taken as defining the shape of the mechanism at failure.

18. The load–deflexion plot with $\beta = 35{\cdot}5°$ is drawn in Fig. 7 for various values of l/b; as expected, the higher aspect ratio mechanisms carry higher loads (because of lengthening of the yield lines). For the value of β chosen, the load–deflexion plot passes through unity on the normalized load axis.

19. Examination of specimen plates (Figs 1 and 2) shows the central ridge of the mechanism to have a sensibly constant width of $0{\cdot}5b$. If this value is assumed to hold for the theoretical straight line mechanism, EF in Fig. 3, with an angle β of 35·5° the aspect ratio may be deduced to be 0·7. This is consistent with the experimental evidence of Figs 1 and 2 which show the curved yield lines of the real mechanism to be $0{\cdot}5b$ apart at the edges of the plate and approximately b apart in the centre, and may be viewed as upper and lower bounds on the theoretical mechanism length.

20. Moxham[2] in his analysis of plate behaviour adopted an aspect ratio of 0·875 for his theoretical elasto-plastic model and noted that his analysis indicated the whole behaviour of the plate to be insensitive to this aspect ratio. It is therefore significant to observe the sensitivity of the load–deflexion curves of Fig. 7 to the aspect ratios of a theoretical yield line model.

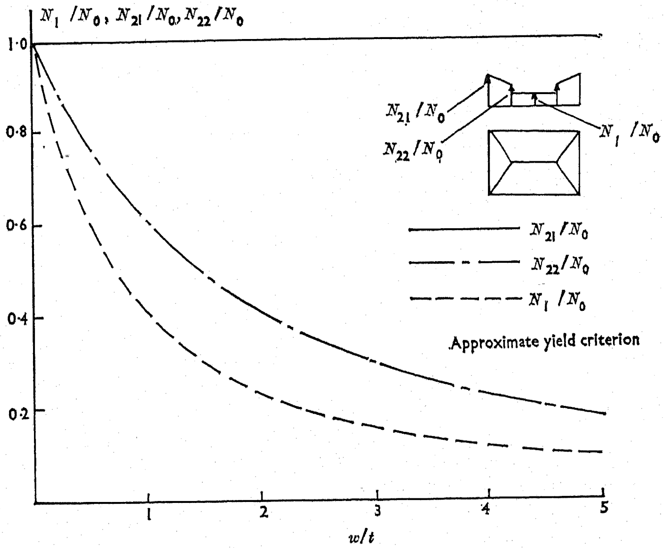

Fig. 8. Load distribution across mechanism

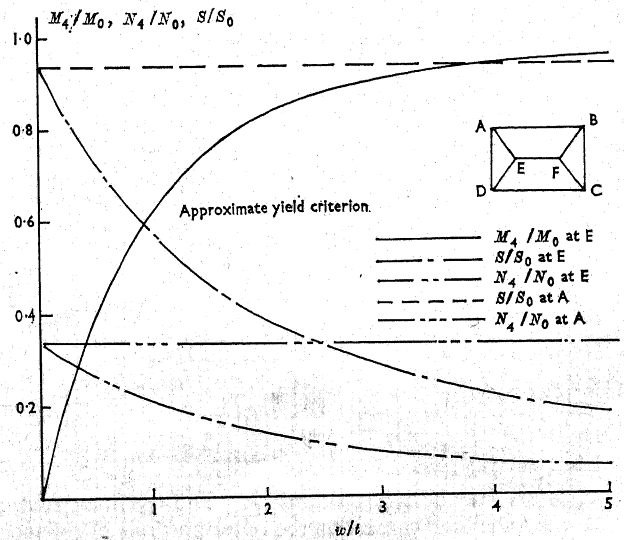

Fig. 9. Bending, shear and axial forces on inclined yield lines

21. As fixed values have now been adopted for both l/b and β, the locus of failure loads of the mechanism for increasing values of the pre-failure deformation w_0 is identical with the subsequent unloading line of the plate after failure. This unique line is found from equation (16) which may now be re-written with these specified values of l/b and β as

$$\sigma^* = 0{\cdot}5\left\{\left[1+\left(\frac{w}{t}\right)^2\right]^{1/2}-\frac{w}{t}\right\}+0{\cdot}25\left[1+0{\cdot}25\left(\frac{w}{t}\right)^2\right]^{1/2}+\frac{0{\cdot}49}{(w/t)}\log\left\{0{\cdot}5\frac{w}{t}+\left[1+0{\cdot}25\left(\frac{w}{t}\right)^2\right]^{1/2}\right\}-0{\cdot}13\frac{w}{t} \quad . \quad . \quad . \quad (17)$$

22. The constant value of N_1 and the boundary values of N_2 are plotted in Fig. 8 to give an indication of the load distribution across the mechanism. As expected, the outer edges of the plate carry the greatest proportion of the load with the edge load being at the yield axial force $N_2/N_0=1$. This distribution has a discontinuity at the junction of the edge and centre strips due to the change in yield line direction of the straight line approximation to the actual curved yield lines.

23. Values of the membrane force N_4, the shear force S and the moment M_4 at the points A and E on the inclined yield lines are plotted in Fig. 9. The moment at A is zero and at E the value increases from zero with increasing deflexion. At zero deflexion the normalized shear force S/S_0 at both A and E has a very high value of 0·94, although at E this value falls with increasing deflexion; this shows the prime importance of the shearing force in the formation of the mechanism. These high values of shear have been suggested by Murray.[10]

Full yield criterion

24. The use of the approximate yield criterion equation (5) results in a simple explicit formulation relating the load to the deflexion of the plastic mechanism. However, the fact that very high shear stresses are present in the mechanism must throw doubt on the validity of the approximate yield criterion. The full yield criterion is used in the following analysis, but unfortunately, although the results are obviously more reliable, they cannot be expressed in a simple form.

25. The full yield criterion equation (4) is now substituted into the solution of the equilibrium equations (10)–(12) for the edge strips. Solution of these equations leads to the following polynomial in N_2/N_0

$$4\sin^2\beta\cos^2\beta\left(\frac{N_2}{N_0}\right)^6+64\frac{x}{l}\frac{w}{t}\sin\beta\cos^3\beta\left(\frac{N_2}{N_0}\right)^5+\left[256\left(\frac{x}{l}\right)^2\left(\frac{w}{t}\right)^2\cos^4\beta-1+\sin^4\beta+16\cos^4\beta\right]\left(\frac{N_2}{N_0}\right)^4-16\frac{x}{l}\frac{w}{t}\cot\beta\times(1+4\sin^2\beta\cos^2\beta)\left(\frac{N_2}{N_0}\right)^3-4\cot^2\beta\left[16\left(\frac{x}{l}\right)^2\left(\frac{w}{t}\right)^2+2-\sin^4\beta\right]\left(\frac{N_2}{N_0}\right)^2+16\frac{x}{l}\frac{w}{t}\cot\beta\frac{N_2}{N_0}+\operatorname{cosec}^4\beta-1=0 \quad . \quad . \quad . \quad (18)$$

26. This equation may be solved numerically and the integrated values of N_2/N_0 found to give the load carried by the outer portions of the mechanism. The total load carried by the mechanism may then be found as previously.

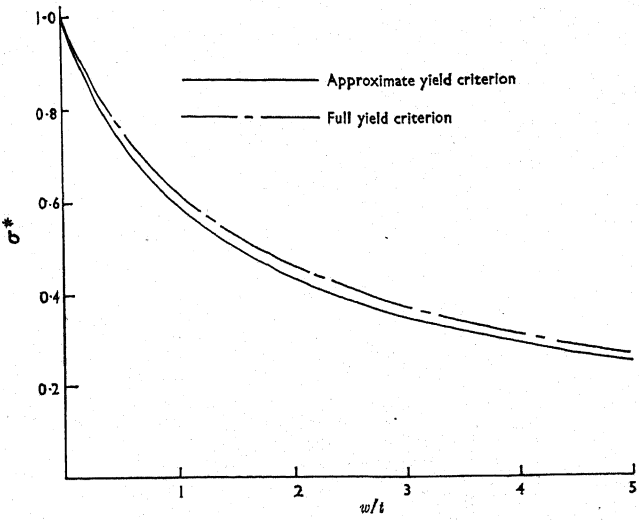

Fig. 10. Comparison of unloading lines

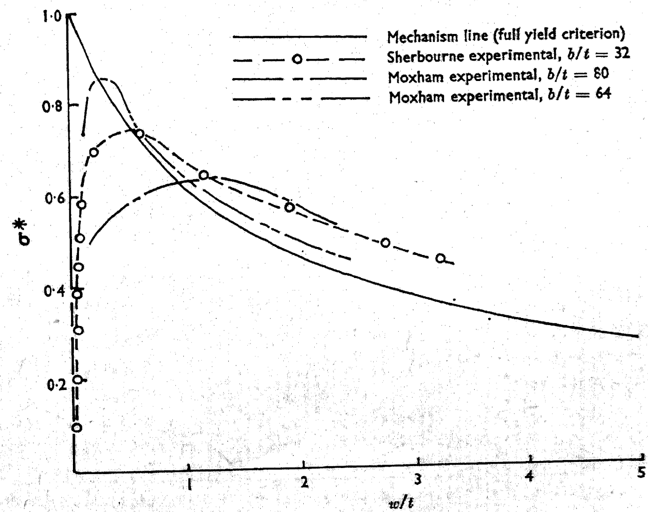

Fig. 11. Theoretical plotted against experimental behaviour

Minimization of the load for various values of w_0 gives values which are shown in Fig. 6 to be close to those obtained using the approximate yield criterion. Again the minimum value of β for which the implicit inequalities of the yield criterion hold is 35·5°.

27. The load–deflexion plot is drawn in Fig. 10 for this value of β and an aspect ratio of 0·7, and is seen to lie slightly above equation (17), indicating an increase in load-carrying capacity. The normalized shear force at A (S/S_0) may again be calculated and has the high value of 0·94: identical to that found using the approximate yield criterion and again being the dominant term in the formation of the inclined yield lines.

Comparison with experiments

28. Curves of experimental load against out of plane deflexion for tests on simply supported metal plates are drawn in Fig. 11. The Moxham[11] tests shown are for steel plates with b/t ratios of 64 and 80 and with aspect ratio of 4. The Sherbourne and Korol[7] test is for a square tube of structural aluminium alloy with a b/t ratio of 32 and an aspect ratio of 3. Allowing for variations in yield strength and the neglect of the strain hardening modulus noted by Moxham in his test plates, the theoretical unloading curve using the full yield criterion is a good lower fit on the experimental plots, and provides an accurate indication of their post-failure behaviour.

29. A rigid–plastic analysis may be expected to yield an upper bound on the experimental plots; however, it is in the nature of the strip approach to neglect various forces and moments which act in the real plate during the deflexion process. In particular, the transverse incompatibility of the mechanism of Fig. 3 and the consequent assumption of zero twisting moments on the inclined yield lines may be a small but significant omission.

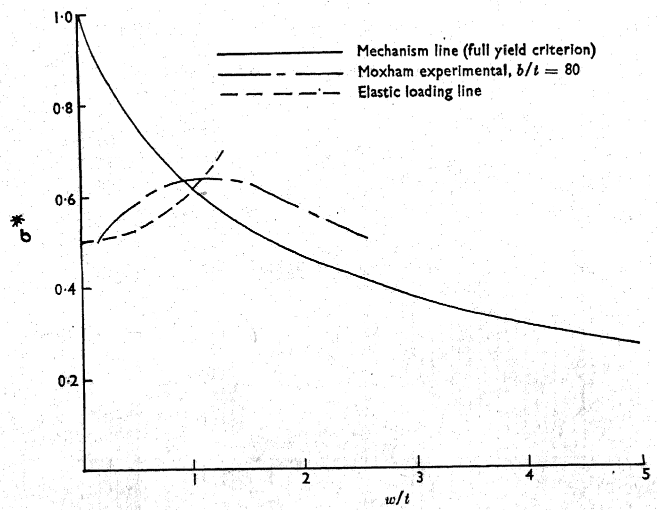

Fig. 12. Prediction of failure load

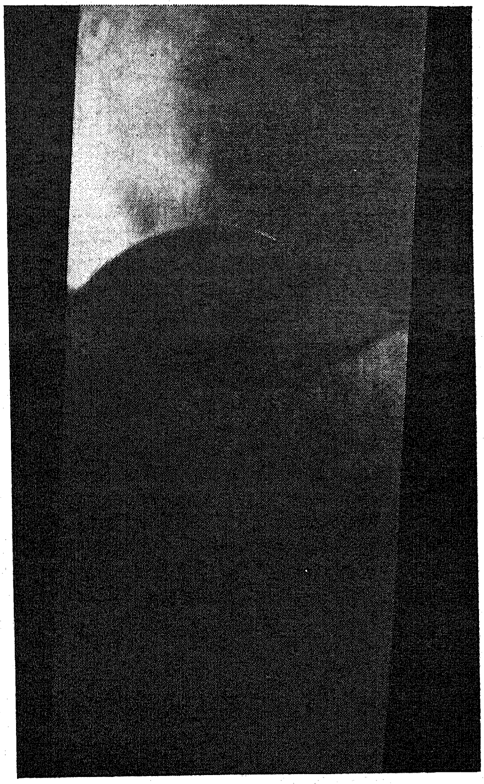

Fig. 13

30. In Fig. 12 one of the Moxham experimental plots ($b/t = 80$) is redrawn, together with the unloading line using the full yield criterion and a theoretical elastic loading path for an analysis by Walker[12]; because of the extreme flatness of Moxham's test plates the perfect plate loading path is taken. The intersection of the elastic loading and the plastic unloading lines gives a prediction of ultimate load within 5% of the measured test value.

Other yield mechanisms

31. Although the pitched roof mechanism presented consistently occurs for axially loaded plates within the low and medium b/t range, it is possible for other yield shapes to occur. Under identical loading and support conditions an elliptical mechanism is able to form within the length of a very thin plate because of the elastic flexibility of the areas of plate on either side of the mechanism. Such a mechanism (Fig. 13) was observed in a test at University College, London on a simply supported steel plate with a b/t of 112. This mechanism has also been noted by Dwight and Harrison[13] in their box column tests and by Watson and Babb.[14]

32. Analysis of this mechanism using the strip approach would not provide

a realistic unloading curve because the elastic contribution to the overall energy of deformation would be neglected.

Conclusions

33. A simple strip analysis of a plate mechanism has been presented which accurately predicts the unloading path of a simply supported plate under uniaxial compression. The importance of shearing forces on the formation and behaviour of the mechanism has been shown, as has the necessity for including these in the yield criterion. The prediction of ultimate carrying capacity has also been shown possible by intersection with a theoretical elastic loading line. The validity of the rigid–plastic approach for the analysis of other buckling problems under various loading and edge conditions has been indicated, and the Paper shows the feasibility of developing this theory further to provide accurate design information.

References

1. GRAVES-SMITH T. R. *The ultimate strength of locally buckled beams of arbitrary length.* PhD thesis, Cambridge University, 1966.
2. MOXHAM K. E. *Theoretical prediction of the strength of welded steel plates in compression.* Cambridge University, 1971, Technical report CUED/C-Struct/TR-2.
3. CRISFIELD M. A. *Large deflection elasto-plastic buckling analysis of plates using finite elements.* Transport and Road Research Laboratory, 1973, Report LR 593.
4. DEAN J. A. *The collapse behaviour of steel plating subject to complex loading.* PhD thesis, Imperial College, London, 1975.
5. ROCKEY K. C. and SKALOUD M. The ultimate load behaviour of plate girders loaded in shear. *Struct. Engr*, 1972, **50**, 29–47.
6. CALLADINE C. R. *A plastic theory for collapse of plate girders under combined shearing force and bending moment.* Cambridge University, 1972, Technical report CUED/C-Struct/TR-29.
7. SHERBOURNE A. N. and KOROL R. M. Ultimate strength of plates in uniaxial compression. *National Structural Meeting*, 1971. American Society of Civil Engineers, New York, 1971.
8. WALKER A. C. and MURRAY N. W. A collapse mechanism for compressed plates. *Int. Assn Bdge Struct. Engng*, 1975, **35**, 217–236.
9. MURRAY N. W. Das aufnehmbare moment in einem zur richtung der Normalkraft schräg liegenden plastichen Gelenk. *Bautechnik*, 1973, **2**, 57–58.
10. MURRAY N. W. Buckling of stiffened panels loaded axially and in bending. *Struct. Engr*, 1973, **51**, 285–301.
11. MOXHAM K. E. *Buckling tests on individual welded steel plates in compression.* Cambridge University, 1971, Technical report CUED/C-Struct/TR-3.
12. WALKER A. C. The post-buckling behaviour of simply-supported square plates. *Aeronaut. Q.*, 1969, **20**, 203–222.
13. DWIGHT J. B. and HARRISON J. D. *Local buckling problems in steel beams.* British Welding Research Association, 1963, Report M9/63.
14. WATSON C. and BABB A. S. *Box columns; progress report on the determination of stiffening requirements.* British Steel Corporation (Swinden Laboratory), 1968, Report DTS.68/718/A.